Journal of Southeast University (English Edition) Vol. 32, No. 1, pp. 78 - 84 Mar. 2016 ISSN 1003—7985

Critical load position for cavities beneath CRCP slab under vehicle loading

Chen Xiaobing Zhao Ronglong Tong Jinhu Huang Xiaoming Luo Ruilin

(School of Transportation, Southeast University, Nanjing 210096, China)

Abstract: In order to study the critical load position that causes cavities beneath the continuously reinforced concrete pavement (CRCP) slab under vehicle loading, the elliptical load is translated into the square load based on the equivalence principle. The CRCP slab is analyzed to determine the cavity position beneath the slab under vehicle loading. The influences of cavity size on the CRCP slab's stress and vertical displacement are investigated. The study results show that the formation of the cavity is unavoidable under traffic loading, and the cavity is located at the edge of the longitudinal crack and the slab corner. The cavity size exerts an obvious influence on the largest horizontal tensile stress and vertical displacement. The slab corner is the critical load position of the CRCP slab. The results can be used to assist the design of CRCP in avoiding cavities beneath slabs subject to vehicle loading.

Key words: vehicle loading; cavity; continuously reinforced concrete pavement (CRCP); critical load position; finite element method (FEM)

DOI: 10.3969/j.issn.1003-7985.2016.01.014

Continuously reinforced concrete pavement (CRCP) is a good kind of rigid pavement structure with continuous longitudinal steel reinforcement but with no preventive measures for contraction joints or transverse expansion[1].

It is well known that the CRCP cracks are usually caused by temperature drops and water evaporation in cement concrete[2-4]. Repetitive vehicle loading and thermal loading force the concrete slab to crack vertically. The closely spaced transverse cracks and longitudinal joints cause punchouts failure[5-7]. Therefore, the CRCP punchouts are proposed as the basic design parameter for CRCP in the Guide for Mechanistic-Empirical Design[8]. The punchouts of CRCP are usually related to the cavities of CRCP. Therefore, it is practically significant to analyze the cavity position beneath the slab under vehicle loading of CRCP.

In this paper, the vehicle loading is translated into the square load according to the equivalence principle first. Secondly, the finite element model is established and the reliability of the model is verified. Next, the cavity positions are analyzed using the FEM. The effects of cavity dimension on the maximum tensile stress and maximum vertical displacement of CRCP slab are analyzed. Finally, the critical load position is suggested. These analysis results are helpful for the study and design of CRCP considering the adverse factor of cavity foundation under vehicle loading.

1 Simulation of Load Transfer and Vehicle Loading

1.1 Simulation of crack's load transfer

The spring element is used to simulate the crack's load transfer[9]. The load transfer efficiency of the crack is simulated using horizontal, vertical and longitudinal springs in the model. The crack model is shown in Fig. 1.

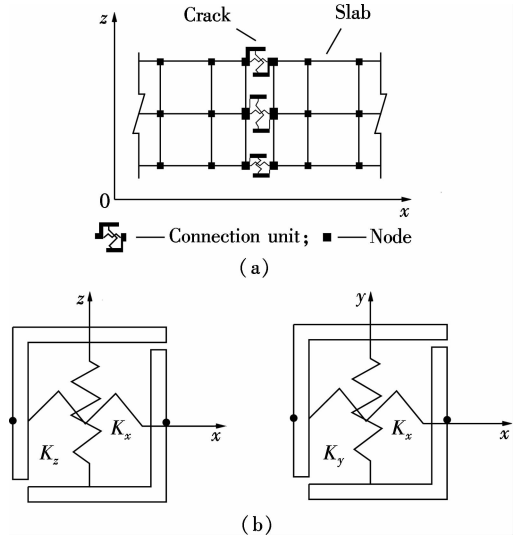

Fig. 1 Crack model and connection unit model. (a) Crack model; (b) Connection unit model

1.1.1 The load transfer of longitudinal steels

The connection rigidity of longitudinal steels' position in the crack section is composed of K_x, K_y, K_z. K_x (connection rigidity in x) is the extensional rigidity of steel. K_y and K_z (connection rigidity in y and z) are the shear rigidity under the combined work of steel and concrete at

Received 2015-09-23.

Biography: Chen Xiaobing (1973—), male, doctor, associate professor, xbchen@seu.edu.cn.

Foundation item: The Science Foundation of Ministry of Transport of the People's Republic of China (No. 200731822301-7).

Citation: Chen Xiaobing, Zhao Ronglong, Tong Jinhu, et al. Critical load position for cavities beneath CRCP slab under vehicle loading[J]. Journal of Southeast University (English Edition), 2016, 32(1): 78 - 84. DOI: 10.3969/j.issn.1003-7985.2016.01.014.

the crack, which is composed of S_{cs} (the shear rigidity resulting from the support of concrete to steel) and S_s (the shear rigidity of longitudinal steel). The steel stiffness of the specific composition is shown in Tab. 1.

Tab. 1 Steel stiffness definition of load transfer

Direction	Stiffness	Remark
Tangential	$S_{com}=\dfrac{1}{\dfrac{1}{S_{cs}}+\dfrac{1}{S_s}}$	$S_{cs}=\dfrac{4\beta^3 E_s I_s}{2+\beta w_{cr}},\ \beta=\left(\dfrac{K_{sc}d}{4E_s I_s}\right)^{1/4}$ $S_s=\dfrac{12E_s I_s}{w_{cr}^3(1+\varphi)},\ \varphi=\dfrac{12E_s I_s}{G_s A_{se} w_{cr}^2}$
Longitudinal	$K_x=E_s A_{sc}/w_{cr}$	

In Tab. 1, β is the rigidity of steel relative to concrete; K_{sc} is the support modulus of concrete to steel; E_s is the elasticity modulus of steel; I_s is the inertia moment of steel section; G_s is the sheer modulus of steel; A_{se} is the effective section area of steel; d is the diameter of steel; w_{cr} is the crack width.

1.1.2 The load transfer of concrete crack

The nodes of the crack section can be divided into nodes in the slab corner, nodes in the slab edge and nodes in the slab center. The crack rigidity distribution at the concrete's three types of positions is allocated according to the area contribution of nodes, which is shown in Fig. 2. Three kinds of nodes' area contributions and the computational formulae of node spring element rigidity are shown in Tab. 2.

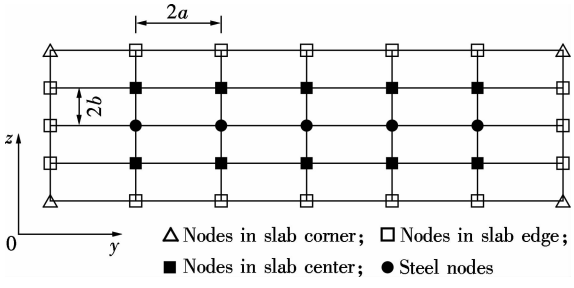

Fig. 2 Diagram of node stiffness distribution

Tab. 2 Computational formula of node stiffness

Position	Contribution area	Number of nodes	Node stiffness
Slab corner	ab	4	$\dfrac{qL_c}{4(N_c N_r-N_c-2N_r+3)}$
Slab edge	$2ab$	$2(N_c+N_r-4)$	$\dfrac{2qL_c}{4(N_c N_r-N_c-2N_r+3)}$
Slab center	$4ab$	$4(N_c-2)(N_r-3)$	$\dfrac{4qL_c}{4(N_c N_r-N_c-2N_r+3)}$

In Tab. 2, the parameter q is the load transfer rigidity of aggregate occlusion; L_c is the crack length; N_c is the number of node lines in the crack section; N_r is the number of node rows in the crack section.

1.2 Vehicle loading simulation

The applied loading is the standard axle load (BZZ-100). The tire pressure is 0.7 MPa and the dual tire load weight is 50 kN. It is assumed that the vehicle loading is evenly distributed in the contact surface, and the size of the contact area is related to the contact pressure. The shape of the contact area between the pavement and wheels contains two half circles and one rectangular as shown in Fig. 3[9]. The contact area A_{act} is calculated as

$$A_{act}=\pi(0.3L)^2+(0.4L)(0.6L)=(0.09\pi+0.24)L^2 \tag{1}$$

$$L=\sqrt{\frac{A_{act}}{0.09\pi+0.24}}=\sqrt{\frac{F/p}{0.09\pi+0.24}} \tag{2}$$

where L is the length of a wheel track; F is the single-wheel weight; P is the single-tire pressure.

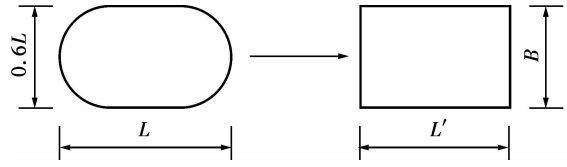

Fig. 3 Diagram of load area transformation

For the ease of calculation, the elliptic contact area can be further simplified as a single rectangle ($L'\times B$).

$$L'=\frac{A_{act}}{B}=\frac{0.09\pi+0.24}{0.6}L \tag{3}$$

As a calculation result, $L'=0.228$ m and $B=0.157$ m. Taking the simplicity of messing and the physical condition of the load transverse distribution into consideration, the values of the standard load equivalent area and transverse distribution are shown in Fig. 4.

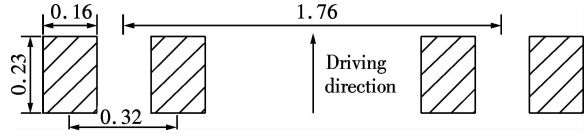

Fig. 4 Distribution of load area (unit: m)

2 Finite Element Model and Its Verification

2.1 Basic assumptions

Considering the efficiency of the crack load transfer of CRCP, the following assumptions are proposed for the FEM[9]:

1) The longitudinal steels are regularly established along the vehicle's direction of movement. They are completely bonded between concrete and steels with compatible deformations. The reinforcement of the transverse steels is ignored. The layers of the pavement are homogeneous, continuous, isotropic and elastic structures.

2) The deflection of the concrete panel is far less than the panel thickness, so the slab warpage is a small-deflection bending problem.

3) The transverse crack is perpendicular to the traffic direction.

4) There is complete contact between the pavement and basement without friction, which means that the pavement can slide along but not separate from the basement.

2.2 Ground model and boundary conditions

Usually, the Winker foundation model is adopted to analyze the clumpy slab system considering the load transfer efficiency in the FEM[9].

Clamped boundary conditions are set at both ends of the two lateral slabs along the moving vehicle's direction, and the displacement of the longitudinal steels is zero in the *x*-axis direction.

2.3 Model size

The crack distance of the middle slab, which is the main object in this study, is 0.6 m. The three-dimensional finite element model of three slabs is established. The length of each side slab is 3 m. It is assumed that the crack width is 0.5 mm. Cao's research shows that the slab width has a little effect on stress and deflection[10]. Therefore, the slab width is uniformly set to be 4 m and the slab thickness is 24 cm. Longitudinal steels are placed in the middle thickness of slabs with a steel ratio of 0.66% and the spacing is 16 cm.

2.4 Finite element unit selection and meshing

The CRCP slab is meshed into 20-node hexahedron secondary reduced integral units (C3D20R). The sizes of the finite element model in the horizontal direction are 8 cm × 6 cm (middle slab) and 8 cm × 10 cm (both side slabs), respectively. The slab is divided into four layers in thickness. The basement is meshed into eight-node linear hexahedron reduced integral units that are C3D8R. The width and length of the basement element are 8.8 and 7.3 cm, respectively. The basement is divided into three layers in thickness (see Fig. 5).

2.5 Structural material parameters

The strength of the concrete is C40 level. HRB335 twisted steels are used as the longitudinal steels. The material parameters[9] are presented in Tab. 3.

2.6 Determination of load position

Wheel load is applied at the middle of the transverse crack edge, slab corner, middle of the longitudinal crack edge and slab center, respectively, as shown in Fig. 6.

2.7 Model verification

The crack rigidity coefficient J_c is adjusted to meet the computation results of LTE_w (the vertical displacement load transfer efficiency) calculated by ABAQUS and AASHTO2002[8], respectively. The calculation result is reliable as shown in Fig. 7.

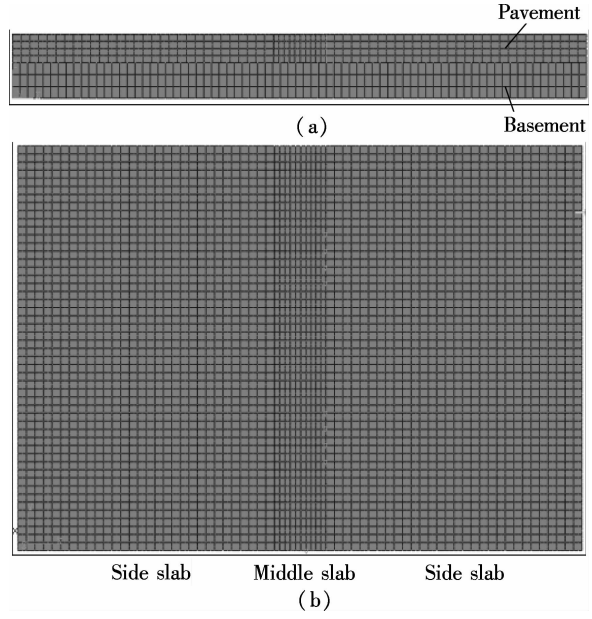

Fig. 5 Finite element model of pavement structure. (a) Diagram of pavement structure layers; (b) Floor plan

Tab. 3 Material parameters

Material	Reaction modulus/(MPa · m^{-1})	Young's modulus/GPa	Poisson's ratio
Concrete		31	0.15
Steel		200	0.30
Basement		2	0.20
Winkler foundation	50		

3 Cavities Beneath Slab

Cavities occur under the combined actions of vehicle loading and interlayer stagnant water underneath the slab. Cavities underneath the slabs of concrete pavement refer to the formation of voids between the slab and the base.

3.1 Formation mechanism and influence factors of cavity

Based on the cause and process of cavity formation, cavities can be divided into two types: the structural cavities and pumping cavities. It is generally considered that the incipient cause of cavities is the accumulation of plastic deformation of the pavement slab where the vertical displacement is relatively large under cyclic vehicle loading[9]. Subsequently, rain infiltrates below the CRCP slab through cracks and gaps between slabs and forms high-pressure water under vehicle loading. Under this condition, high-pressure water that flows through the edges of slabs and cracks in the underside of slabs at high speed will result in base erosion and base material loss until forming the cavity.

There are many factors which influence the formation of cavities[11]. According to the sources of these factors, they can be divided into external factors and internal factors.

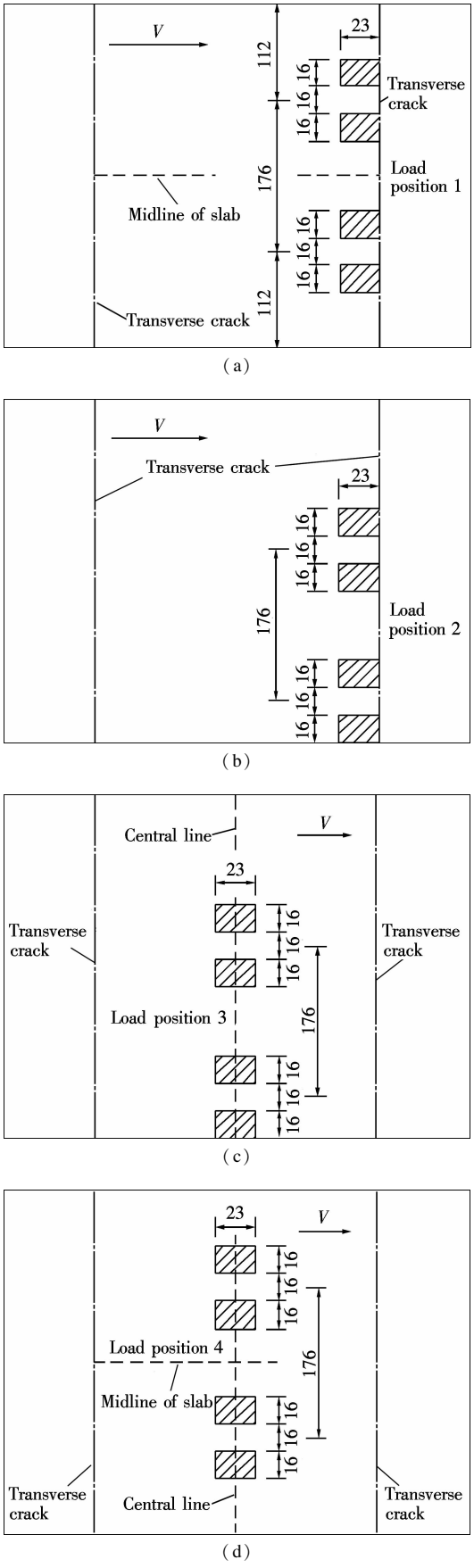

Fig. 6 Load position of middle slab (unit: cm). (a) Load applied at the middle of the transverse crack edge; (b) Load applied at the slab corner; (c) Load applied at the middle of the longitudinal crack edge; (d) Load applied at the slab center

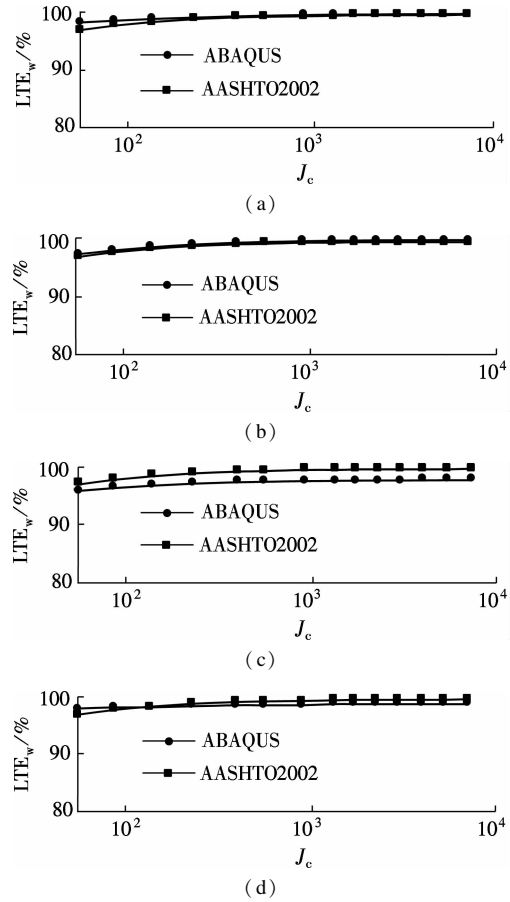

Fig. 7 Diagram of model verification. (a) Load applied at the middle of the transverse crack edge; (b) Load applied at the slab corner; (c) Load applied at the middle of the longitudinal crack edge; (d) Load applied at the slab center

External factors include the natural environment, vehicle loading and the rules that traffic keeps to the right. Internal factors include the structural characteristics of CRCP, properties of concrete slabs, properties of base materials, transverse gradient of pavement, drainage performance of pavement and subgrade, and construction quality[9].

3.2 Possible locations of the cavity areas

3.2.1 Influences of vehicle loading positions

The vertical displacement of the CRCP slab is closely related to the vehicle loading position[9]. In general, the vehicle moving from one side to the other side of the middle slab in the driving direction has the following paths:

1) The wheel moves along the slab longitudinal edge.

2) The wheel has some distance from the slab longitudinal central line.

3) The wheels are symmetrical to the slab longitudinal central line.

The computational model is a three-slab system. The parameters of the pavement structure and material are the same as mentioned before. During the process of analysis, the standard axle load (BZZ-100) moves along the x-coordinate axis and y-coordinate axis. The central section of the outmost edge of the wheel path is chosen as

the datum point. The datum point moves to six load positions in sequence. These load positions are numbered from 1 to 6, respectively, which are six kinds of wheel load position: ($x=0.115$ m, $y=0$ m), ($x=0.115$ m, $y=0.400$ m), ($x=0.115$ m, $y=0.880$ m), ($x=0.300$ m, $y=0$ m), ($x=0.300$ m, $y=0.400$ m), ($x=0.300$ m, $y=0.880$ m) (see Fig. 8). The maximum vertical displacement at each load position is calculated. The results are shown in Tab. 4.

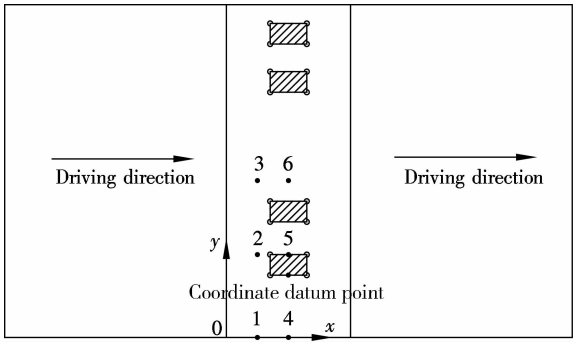

Fig. 8 Diagram of load position moving along x, y directions (unit: m)

Tab. 4 The maximum vertical displacement

x/m	$w_{L,max}$/mm		
	$y=0$ m	$y=0.400$ m	$y=0.880$ m
0.115	0.830	0.631	0.557
0.300	0.769	0.581	0.516

As shown in Tab. 4, the maximum vertical displacement is at the slab corner ($x=0.115$ m, $y=0$ m). It is 1.6 times larger than the minimal value at the slab center ($x=0.300$ m, $y=0.880$ m).

3.2.2 Influence of lateral distribution of wheel path

Load position and especially the frequency of repeated vehicle loading have a great influence on the positions and severity of cavities. The frequency of the wheel path lateral distribution at the edge of the lane is higher, which indicates a higher frequency of repeated vehicle loading[9]. Therefore, the edge of the lane is more prone to have cavities.

3.2.3 Highest possible locations of the cavity areas

Based on the analysis of the wheel path lateral distribution law and positions of maximum vertical displacement, we can infer that the cavity is most likely to emerge at the slab corner. Deflection in ranges of both sides of transverse and longitudinal edges of the slab is also relatively large. In these ranges, the formation of cavities is caused by plastic deformation and erosion of the base.

3.3 Basic shapes and types of cavity

3.3.1 Basic shapes of cavity

The cavity areas underneath the pavement slab are usually symmetric for the transverse cracks. The cavity space can be considered as a triangular wedge. The closer to the slab center, the smaller the cavity depth; in contrast, the closer to the slab corner, the larger the cavity depth. Domestic documentation on investigation and repair of the cavity underneath the cement concrete pavement slab shows that the shape of the cavity underneath the corner of the slab is approximately circular or triangular. The shape of the cavity area underneath the pavement slab is an isosceles right triangle[12-13]. The overview of the pavement with cavity areas is shown in Fig. 9.

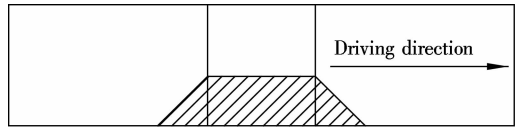

Fig. 9 Planform of cavity underneath slab

3.3.2 Influence of cavity dimension on mechanical response

Six sizes of the cavity area are provided as 0.2 m × 0.2 m, 0.4 m × 0.4 m, 0.6 m × 0.6 m, 0.8 m × 0.8 m, 1.0 m × 1.0 m and 1.2 m × 1.2 m. Nine cavity depths are provided as 0.05, 0.1, 0.2, 0.3, 0.6, 0.9, 1.2, 1.5 and 1.8 mm. The influences of plane dimension and depths of the cavity on the mechanical response of the load-bearing slab are analyzed as comparisons. During the process of analysis, the load is applied at the corner of the middle slab (see Fig. 6(b)). The thickness of the pavement is 24 cm, the thickness of the basement is 30 cm, the foundation reaction modulus is 50 MPa/m, and the interface contact between the pavement and the basement is assumed to be completely smooth.

The variations of both the maximum horizontal tensile stress σ_y and the maximum vertical displacement w_L along the width direction of the load-bearing slab with plane dimension as well as depths of cavities are shown in Fig. 10.

From Fig. 10, the following conclusions can be drawn:

1) The plane dimension of the cavity underneath the slab has a remarkable influence on the maximum tensile stress σ_y and the maximum vertical displacement w_L of the load-bearing slab.

2) The influence of depths of the cavity underneath the slab on the maximum tensile stress σ_y and the maximum vertical displacement w_L of the load-bearing slab is insignificant.

3) Depths of cavity underneath the slab have insignificant effects on the load stress of pavement. Therefore, the influence of the plane dimension of the cavity should be taken into consideration as a major factor in the following analysis.

3.4 Estimation of cavity dimension

The formation of the cavity is closely related to rainfall, the properties of base materials, and the frequency

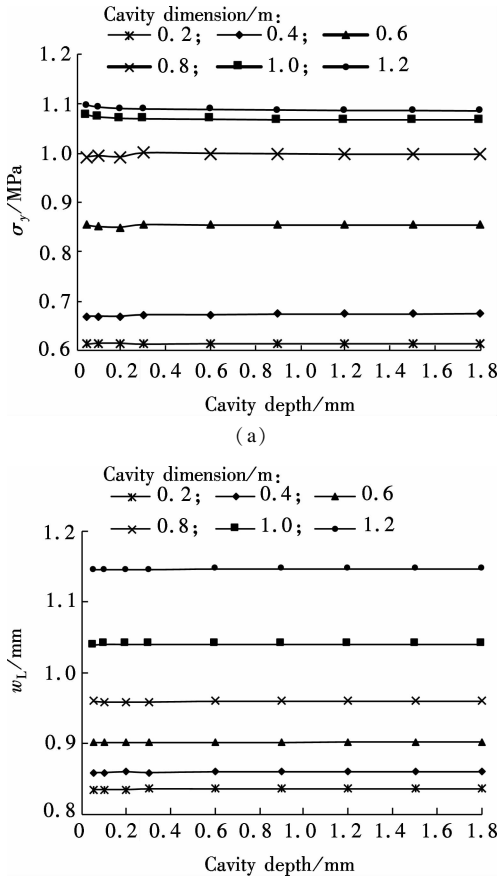

Fig. 10 Effects of cavity depth on maximum tension stress σ_y and maximum vertical displacement w_L. (a) σ_y; (b) w_L

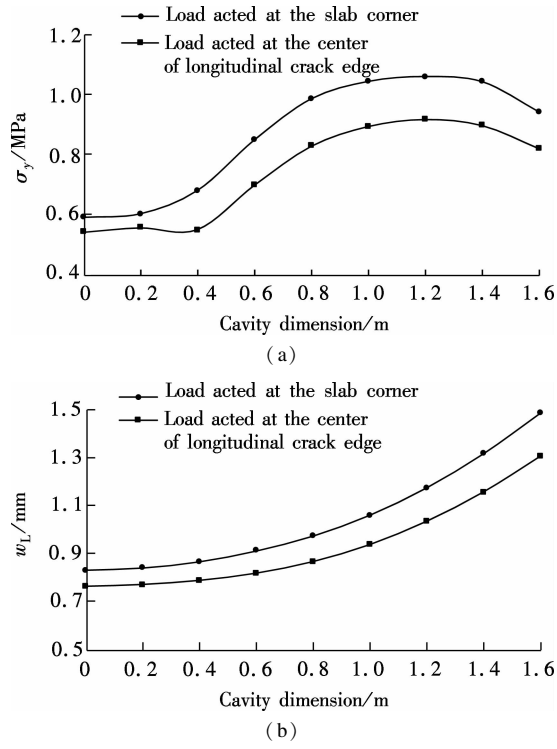

Fig. 11 Effects of cavity dimension on maximum tension stress σ_y and maximum vertical displacement w_L. (a) σ_y; (b) w_L

of repeated vehicle loading. AASHTO has proposed a prediction model of the cavity underneath the edge of the slab which takes into account both rainfall and properties of base materials. The model is described as[8]

$$V_i = V_{i-1} + E_i \qquad i = 1,\ V_i = 0 \tag{4}$$

$$E_i = 0.025\,4(-0.37 + 0.017P_{200} + 0.077\,9I_{\text{void}} + 0.460\,6R_i \tag{5}$$

where V_i is the total cavity dimension at the end of the year i; E_i is the cavity dimension of the year i; P_{200} is the passing ratio of base materials at 0.075 mm sieve; R_i is the average precipitation of the year i; I_{void} is the cavity index.

4 Critical Load Position of Cavity Slab

The two sets of vehicle positions, slab corner and middle of the longitudinal crack edge, are simulated for the finite element model as shown in Figs. 6(b) and (c).

The maximum tensile stress σ_y and the maximum vertical displacement w_L under the vehicle loading in different positions are calculated as shown in Fig. 11.

The positions of the horizontal maximum load stress with other cavity dimensions are similar to those in Fig. 12, and only the load stress values are different.

From Fig. 11 and Fig. 12, the following conclusions can be drawn:

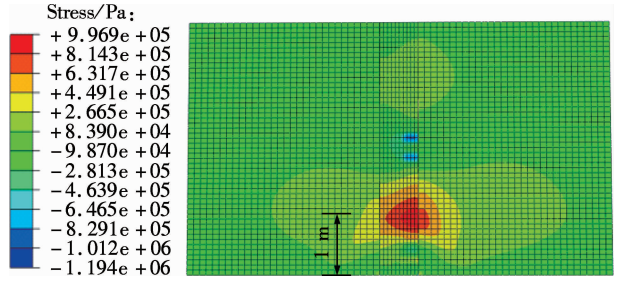

Fig. 12 The position of the maximum tension stress with a cavity dimension of 0.8 m

1) The position of the horizontal maximum tensile stress σ_y of the cavity slab is around 1.0 m from the slab top, which is consistent with the punchout position in the actual pavement.

2) When the load is applied at the slab corner and the middle of the longitudinal crack edge, the cavity dimension has a great influence on the horizontal maximum tension stress. The horizontal maximum tension stress reaches its summit when the cavity size is 1.2 m. Slab corner is the unfavorable load position for the maximum horizontal tension stress.

3) The cavity dimension has a great influence on the maximum vertical displacement of the two load positions. Corner loading leads to larger maximum vertical displacements. Slab corner is the unfavorable load position for the maximum vertical displacement.

According to the above analysis, the slab corner is the critical load position of the maximum tensile stress and the maximum vertical displacement under the vehicle

loading when there is a possible cavity.

5 Conclusions

1) The cavity underneath the slab is most likely to emerge at the slab corner. The shape of the cavity is close to a triangle.

2) When the load is applied at the slab corner and the middle of the longitudinal crack edge, the cavity dimension has a great influence on the horizontal maximum tensile stress and the maximum vertical displacement. The slab corner is the critical load position of the CRCP slab when a cavity possibly exists.

3) In order to ensure the safety of the structure, the vertical displacement and stress of the slab should be analyzed under vehicle loading which is applied at the slab corner, particularly when the CRCP is designed for soft soil base, loess foundation, liquefied sand and mining subgrade.

References

[1] Zhou W J, Choi P, Saraf S, et al. Premature distresses at transverse construction joints (TCJs) in continuously reinforced concrete pavements [J]. *Construction and Building Materials*, 2014, **55**: 212 - 219. DOI:10.1016/j.conbuildmat.2014.01.042.

[2] Choi S, Ha S, Won M C. Horizontal cracking of continuously reinforced concrete pavement under environmental loadings [J]. *Construction and Building Materials*, 2011, **25**(11): 4250 - 4262. DOI:10.1016/j.conbuildmat.2011.04.069.

[3] Kohler E, Roesler J. Active crack control for continuously reinforced concrete pavements[J]. *Transportation Research Record*, 2004, **1900**: 19 - 29.

[4] Ren D Y, Houben L J M, Rens L. Monitoring early-age cracking of continuously reinforced concrete pavements on the E17 at Ghent (Belgium) [C]//*Second International Conference on Sustainable Construction Materials: Design, Performance and Application*. Wuhan, China, 2013: 30 - 41.

[5] Selezneva O, Rao C, Darter M, et al. Development of a mechanistic empirical structural design procedure for continuously reinforced concrete pavements[J]. *Transportation Research Record*, 2004, **1896**: 46 - 56.

[6] Selezneva O, Darter M, Zollinger D, et al. Characterization of transverse cracking spatial variability: Using of LTPP data for CRCP design [J]. *Transportation Research Record*, 2003, **1849**: 147 - 155.

[7] Won M. Identification of CRCP distress mechanisms and calibration of mechanistic-empirical CRCP design procedures with rigid pavement database [C]//*Proceedings of Transportation Research Board 90th Annual Meeting*. Washington, DC, USA, 2011: 51 - 59.

[8] National Cooperative Highway Research Program. Guide for mechanistic-empirical design of new and rehabilitated pavement structures [R]. Chicago, USA: NCHRP 1-37A, 2004.

[9] Chen X B. Structural design method of CRCP based on characteristics of cracking [D]. Nanjing: School of Transportation, Southeast University, 2013. (in Chinese)

[10] Cao D W. Study on structure of continuously reinforced concrete pavement [D]. Xi'an: School of Highway, Chang'an University, 2001. (in Chinese)

[11] Zhao J. Theories and methods for the test and evaluation of hollow underneath rigid pavement slabs [D]. Shanghai: School of Traffic and Transportation, Tongji University, 2006. (in Chinese)

[12] Zhang Q. Study on the cement concrete pavement design considering base erosion and cavity beneath slab [D]. Xi'an: School of Highway, Chang'an University, 2009. (in Chinese)

[13] Wang Q, Han X, Yi Z J. Study on identification of cavity area under concrete pavement using transient impulse-response method [J]. *Journal of Highway and Transportation Research and Development (English Edition)*, 2012, **6**(1): 8 - 14. DOI:10.1061/JHTRCQ.0000083.

车辆荷载作用下脱空连续配筋混凝土路面的临界荷位

陈小兵　赵蓉龙　童金虎　黄晓明　罗瑞林

(东南大学交通学院, 南京 210096)

摘要:为了研究车辆荷载作用下脱空连续配筋混凝土路面的临界荷位,运用等效原理将椭圆形车辆荷载转化为等效的方形荷载,分析了车辆荷载作用下连续配筋混凝土路面板板底易脱空的位置,及脱空尺寸对连续配筋混凝土路面板应力与竖向位移的影响.研究结果表明:车辆荷载作用下连续配筋混凝土路面板板底脱空不可避免,脱空一般位于纵缝边缘与板角位置.脱空尺寸对板的横向最大拉应力和最大竖向位移影响显著,板角为车辆荷载作用下脱空连续配筋混凝土路面的临界荷位.分析结果为脱空的连续配筋混凝土路面的结构设计提供了理论基础.

关键词:车辆荷载;脱空;连续配筋混凝土路面;临界荷位;有限元

中图分类号:U416.216